Journal of Hydrology 534 (2016) 50–62

Contents lists available at ScienceDirect

Journal of Hydrology

journal homepage: www.elsevier.com/locate/jhydrol

Structure and water storage capacity of a small karst aquifer based on stream discharge in southwest China

Tonggang Fu [a,b,c], Hongsong Chen [a,b,*], Kelin Wang [a,b]

[a] Key Laboratory of Agro-ecological Processes in Subtropical Region, Institute of Subtropical Agriculture, Chinese Academy of Sciences, Changsha 410125, China
[b] Huanjiang Observation and Research Station for Karst Ecosystems, Chinese Academy of Sciences, Huanjiang, Guangxi 547100, China
[c] University of Chinese Academy of Sciences, Beijing 100049, China

ARTICLE INFO

Article history:
Received 21 August 2015
Received in revised form 17 December 2015
Accepted 21 December 2015
Available online 30 December 2015
This manuscript was handled by Corrado Corradini, Editor-in-Chief, with the assistance of Bartolome Andreo-Navarro, Associate Editor

Keywords:
Karst
Aquifer structure
Hydrograph
Time series analysis
Effective porosity

SUMMARY

Karst spring/stream discharge reflects the global configuration of the aquifer. However, quantitative description of the aquifer structure such as effective porosity (n_{eff}) and water storage capacity by the discharge analysis is difficult because of the complex conduit/fracture system. This study attempted to quantify the characteristics of karst aquifer based on discharge recession and time series analysis methods. Three recession models, including modified Maillet, Mangin and Boussinesq models, were evaluated to choose the most suitable one for analyzing the aquifer structure, and auto-correlation and cross-correlation functions were applied to study the aquifer response in both year and rainfall event time scales. The results showed that the modified Maillet model was more suitable in the study catchment with Mangin model overestimating and Boussinesq model underestimating the discharge. The n_{eff} was 3.73% for the total aquifer, and it was 0.07%, 0.33% and 3.33% for the conduit, fracture and matrix, respectively. Based on a case study of a rainfall event with precipitation of 68 mm, the water volumes drained by the three media were 25.43%, 33.40% and 41.17%, respectively. This indicates that, although conduit network is not very developed with lower n_{eff}, it is still an important water transmissive element (draining more than a quarter of water after the rainfall event). The memory time of the aquifer was 4 days for the year scale and 8 h for the rainfall event (68 mm) scale. This demonstrates that the aquifer has a well developed drainage system with a quick response to the rainfall. The above results provide further insights for hydrological processes modeling and water resources management for the small catchment in karst regions.

1. Introduction

Karst aquifer always has a dual hydrological system where extremely fast and slow water flow can be found in both saturated and unsaturated zone (Ford and Williams, 2007; Ghasemizadeh et al., 2012; Goldscheider and Drew, 2007; Katsanou et al., 2014; Padilla et al., 1994). High heterogeneity is the most important characteristic of the aquifer where the aperture diameters can vary more than five orders of magnitude from fracture to conduit (Mayaud et al., 2014). Quantitative data of pumping or tracing from points can only provide information of surroundings (Liu et al., 2010; Padilla et al., 1994). As a consequence, global methods, including isotope, absolute gravity, hydrochemistry and many other methods, were widely used to study the overall characteristics and the related hydrological processes of karst aquifer (Aquilina et al., 2006; Hu et al., 2015; Jacob et al., 2008, 2009; Kiraly, 2002; Perrin et al., 2003). However, these methods have disadvantages that more parameters and more expensive instruments are required. By contrast, hydrograph or discharge recession analysis method is simpler because fewer parameters, only discharge data, are needed. Although only hydrograph is considered, similar conclusions, perhaps even more numerous and reliable, can be reached (Bonacci, 1993; Dewandel et al., 2003; Fiorillo, 2014; Tallaksen, 1995).

Since the studies of Boussinesq (1877) and Maillet (1905), discharge recession analysis has become a very popular method to study the hydrological processes and to deduce the aquifer characteristics. The recession analysis was firstly developed to study aquifers with homogeneous structures. However, it was gradually, and then widely, used in karst area with a heterogeneous system as its simplicity (Bonacci, 1993; Chang et al., 2015; Dewandel et al., 2003; Eisenlohr et al., 1997; Fiorillo, 2009; Ghasemizadeh et al.,

* Corresponding author at: Key Laboratory of Agro-ecological Processes in Subtropical Region, Institute of Subtropical Agriculture, Chinese Academy of Sciences, Changsha 410125, China. Tel.: +86 731 84615226.
E-mail address: hbchs@isa.ac.cn (H. Chen).

http://dx.doi.org/10.1016/j.jhydrol.2015.12.042
0022-1694/

2012; Kiraly et al., 1995; Kovács et al., 2005; Padilla et al., 1994; Schmidt et al., 2014). Fiorillo (2014) provided a useful review of the recession analysis and categorized the recession models into empirical, semi-empirical, and physically-based models. Boussinesq, Maillet, and Mangin models are three of the widely used empirical or semi-empirical models (Amit et al., 2002; Eisenlohr et al., 1997; Farlin and Maloszewski, 2013; Lo Russo et al., 2014; Padilla et al., 1994; Schmidt et al., 2014). Boussinesq model (Boussinesq, 1904) is a quadratic equation, but Maillet model (Maillet, 1905) is a simple exponential equation. Both of the two models are used to describe the whole recession process of the discharge from an aquifer, but hardly different flow regimes can be noticed. Karst aquifer is always characterized by different flow media with conduit, fracture and matrix (Forkasiewicz and Paloc, 1967). Therefore, modified Maillet equation, which constituted of several exponential components standing for different flow regimes, was always used (Forkasiewicz and Paloc, 1967; Kovács and Perrochet, 2008). There is no problem that the baseflow is an exponential recession. However, whether the quickflow, which always turbulent flow appeared in the conduit, follows the exponential recession is always questioned. Mangin (1975), for example, pointed out that the exponential equation was not suitable for simulating the quickflow. Based on the Maillet model, he described the discharge recession as a sum of infiltration influenced process (quickflow) and baseflow recession process. Mangin model considered the characteristics of karst aquifer with fast and slow water flows, but one or more intermedia flows may be ignored. As can be seen, these models have both advantages and disadvantages. Moreover, which model can provide better results is still under debate (Dewandel et al., 2003; Lo Russo et al., 2014; Padilla et al., 1994).

The recession coefficient is one of the most important parameters that reflect the aquifer characteristics. Numerous equations were used to calculate this parameter (Boussinesq, 1877; Dewandel et al., 2003; Maillet, 1905). In general, the recession coefficient varies directly with the hydraulic conductivity but inversely with the aquifer storativity (Bonacci, 1993; Fiorillo, 2014; Forkasiewicz and Paloc, 1967; Katsanou et al., 2015; Kiraly, 2002). Different recession coefficients reflect the flow regimes with different hydraulic conductivities (Bonacci, 1993). Therefore, the recession coefficient was always used to describe the development of the conduit network with high hydraulic conductivity, and also to identify the karstification degree of an aquifer (Bailly-Comte et al., 2010; Bonacci, 1993; Ghasemizadeh et al., 2012; Katsanou et al., 2015; Malík and Vojtková, 2012; Padilla et al., 1994; White, 2003). Most of the descriptions were qualitative. However, the quantification of the effective porosity (n_{eff}) and water storage capacity for each hydraulic conductivity media may be more valuable in understanding the aquifer characteristics (Amit et al., 2002; Li, 2009).

Time series analysis is a useful tool for studying the aquifer characteristics. It was firstly used to study karst aquifer by Mangin (1984). Generally speaking, this method includes both univariate (auto-correlation function, ACF) and bivariate (cross-correlation function, CCF) analysis, which could characterize the temporal structure of hydrologic signals under the linear-stationary hypotheses (Labat et al., 2000; Padilla and Pulido-Bosch, 1995). Correlogram, memory time and delay time are always used to describe the karstification degree and the response of the aquifer to the rainfall (Covington et al., 2009; Katsanou et al., 2015; Lo Russo et al., 2014; Mayaud et al., 2014). The existing studies mainly concerned on long time scale (one year or more). Only few considered short time scale (rainfall event or flood scale) (Bailly-Comte et al., 2008; Mayaud et al., 2014). The results of the long time scale reflect the average response of the aquifer to the rainfall, but the short time scale reflect the response of the aquifer to a given pulse (Bailly-Comte et al., 2008; Mayaud et al., 2014). Therefore, it is necessary to study the processes in both time scales. Moreover, the results can be compared with that of the hydrograph analysis to see whether the two methods reflect the same characteristic of the aquifer.

Karst landscape is widely distributed in southwest China with an area of more than 500,000 km^2 (Yuan, 1994). Precipitation in this area is abundant, more than 1000 mm per year. But water resources shortage is still a problem for both ecosystem and human society due to the heterogeneous aquifer and fast hydrological processes (the rapid water flow in both saturated and unsaturated zone), with much water lost through the underground system (Chen et al., 2013; Jiang et al., 2014). Until now, researchers mainly concerned on the hydrological processes of the soil layer (Chen et al., 2010; Li et al., 2014; Zhang et al., 2011). However, the global characteristics of the water storing and transferring in the total aquifer may be more valuable, because soils in this area are always thin and distributed as mosaic with base-rock outcrop widely spread (Chen et al., 2010; Fu et al., 2015b). Therefore, studies should be done to further understand the aquifer structure and the related hydrological processes in this area. Previous study based on isotope method showed a poor development of conduit system and slow hydrological processes (Hu et al., 2015). It is inconsistent with the generally accepted knowledge that extremely fast and slow flow appear in a dual system. Therefore, a new method is needed to verify such results. Hydrograph method, as aforementioned, is a useful way. However, the hydrograph is influenced by the catchment's geomorphologic characteristics, vegetation community and many other environmental factors (Dewandel et al., 2003; Eisenlohr et al., 1997; Gregor and Malík, 2012; Lacey and Grayson, 1998; Lo Russo et al., 2014), all of which are quite unique in southwest China (Chen et al., 2011; Fu et al., 2015a; Nie et al., 2012). As a consequence, the recession models should be evaluated to see which is more suitable in this area.

The purposes of this study were (1) to characterize the hydrograph of the stream and evaluate three recession models (modified Maillet, Mangin and Boussinesq models), (2) to estimate the proportion of conduit, fracture, and matrix and calculate their water storage capacities, and (3) to verify the results with time series analysis method in a small karst catchment in southwest China.

2. Materials and methods

2.1. Recession analysis

Boussinesq (1904) developed a quadratic equation to describe the discharge recession process based on the simplified assumption that the aquifer was porous, free, homogeneous and isotropic:

$$Q_t = \frac{Q_0}{(1+\alpha t)^2} \tag{1}$$

In which Q_0 is the total discharge at $t = 0$ and α is the recession coefficient.

Unlike the Boussinesq model, Maillet (1905) used an exponential equation to simulate the recession process with the following formula:

$$Q_t = Q_0 \times e^{-\alpha t} \tag{2}$$

where Q_t is the discharge at time t, Q_0 is the discharge at $t = 0$, and α is the recession coefficient. In karst area, modified Maillet model was always used and it can be expressed by a sum of several exponential components (Eisenlohr et al., 1997; Fiorillo, 2014; Forkasiewicz and Paloc, 1967; Ghasemizadeh et al., 2012; Tallaksen, 1995):

$$Q_t = \sum_{i=1}^{n} Q_{0i} \times e^{-\alpha_i t} \tag{3}$$

where i represents the media i in the aquifer, Q_{0i} represents the discharge of media i at $t = 0$, and n represents the number of flow components. Karst aquifer can always be divided into conduit, fracture, and matrix systems based on the different hydraulic conductivities (Ghasemizadeh et al., 2012; Katsanou et al., 2015; White, 2003). Therefore, the modified Maillet equation can be written as:

$$Q_t = Q_c \times e^{-\alpha_c t} + Q_f \times e^{-\alpha_f t} + Q_m \times e^{-\alpha_m t} \tag{4}$$

where Q_c, Q_f, Q_m are the initial discharges, and α_c, α_f, α_m are the recession coefficients of the conduit, fracture and matrix, respectively.

Based on Maillet equation, Mangin (1975) concluded that exponential equation was suitable for modeling the baseflow, but not for the quickflow. He calculated the discharge by the following formula:

$$Q_t = \psi(t) + \varphi(t) = Q_q \times \frac{1 - \eta t}{1 + \varepsilon t} + Q_b e^{-\alpha_b t} \tag{5}$$

where $\psi(t)$ and $\varphi(t)$ represent the infiltration function and baseflow function, respectively (El-Hakim and Bakalowicz, 2007). Padilla et al. (1994) pointed out that the value of $\psi(t)$ and $\varphi(t)$ just equals that of fastflow and baseflow. Q_q is the initial infiltration flow rate, and Q_b is the initial baseflow rate. The parameters η and ε mean the infiltration velocity and flow heterogeneity, respectively, and α_b is the baseflow recession coefficient.

The quantitative relationship between recession coefficient and the n_{eff} was given by Fiorillo (2011, 2014):

$$\frac{\alpha_1}{\alpha_2} \approx \frac{n_{\text{eff2}}}{n_{\text{eff1}}} \tag{6}$$

$$\frac{\alpha_2}{\alpha_3} \approx \frac{n_{\text{eff3}}}{n_{\text{eff2}}} \tag{7}$$

where n_{effi} (i = 1–3) means the n_{eff} of different media in the aquifer. Therefore, the n_{eff} of the conduit ($n_{\text{eff-}c}$) and fracture ($n_{\text{eff-}f}$) can be estimated if we know the recession coefficients of the conduit (α_c), fracture (α_f), matrix (α_m) and the effective porosity of the matrix ($n_{\text{eff-}m}$):

$$n_{\text{eff-}f} \approx \frac{\alpha_m \times n_{\text{eff-}m}}{\alpha_f} \tag{8}$$

$$n_{\text{eff-}c} \approx \frac{\alpha_f \times n_{\text{eff-}f}}{\alpha_c} \tag{9}$$

Then the total effective porosity ($n_{\text{eff-}t}$) of the aquifer can be calculated by:

$$n_{\text{eff-}t} = n_{\text{eff-}c} + n_{\text{eff-}f} + n_{\text{eff-}m} \tag{10}$$

Integrating the recession curve over time provides the water storage capacity, that is, water available for drainage from the aquifer (Amit et al., 2002; Farlin and Maloszewski, 2013; Tallaksen, 1995):

$$V_t = \int_0^{t_t} Q_t dt \tag{11}$$

where V_t is the water volume drained at time t. When t approaches infinity, the volume represents the water storage capacity, i.e. the maximum water drained by the aquifer. Accordingly, integrating the recession curve of conduit, fracture or matrix over time provides each water storage capacity.

2.2. Time series analysis

ACF and CCF are widely used in time series analysis. ACF evaluates to what extent does the discharge depends on the preceding values over a specified time period (lag time) (Mayaud et al., 2014). The formula for the ACF is (Eisenlohr et al., 1997; Mayaud et al., 2014):

$$\text{ACF} = \frac{C_k}{C_0} \tag{12}$$

where

$$C_k = \frac{1}{n}\sum_{t=1}^{n-k}(x_t - \bar{x})(x_{t+k} - \bar{x}) \tag{13}$$

and

$$C_0 = \frac{1}{n}\sum_{t=1}^{n}(x_t - \bar{x})^2 \tag{14}$$

where x_t is the discharge value at time t, $\bar{x}$ is the average discharge, n is the total number of the data, and k is the lag time. The memory time, which stands for the lag time when the ACF > 0.2, is used to describe the time that the discharge is influenced by the initial condition (Katsanou et al., 2015; Lo Russo et al., 2014; Mayaud et al., 2014).

The CCF is used to examine the dependence of output series y (discharge) on the input series x (precipitation). It can be calculated by (Mayaud et al., 2014; Padilla and Pulido-Bosch, 1995):

$$\text{ACF} = \frac{C_{xy}}{C_{x0}C_{y0}} \tag{15}$$

where

$$C_{xy} = \frac{1}{n}\sum_{t=1}^{n-k}(x_t - \bar{x})(y_{t+k} - \bar{y}) \tag{16}$$

$$C_{x0} = \frac{1}{n}\sum_{t=1}^{n}(x_t - \bar{x})^2 \tag{17}$$

$$C_{y0} = \frac{1}{n}\sum_{t=1}^{n}(y_t - \bar{y})^2 \tag{18}$$

The symbols have the same meaning with that in the calculation of ACF. The delay time, the lag time between 0 and the time when maximum CCF value appears, can reflect the response time of the aquifer to the rainfall event, and shorter delay time always means faster aquifer transfer (Gárfias-Soliz et al., 2010; Katsanou et al., 2015).

Both of ACF and CCF are always analyzed in correlograms. The steep slope in the correlogram means a fast response of the aquifer to the rainfall and indicates a higher karstification degree. The results can be compared with that of the hydrograph analysis.

2.3. Study area

The study catchment (24°43′58.9″–24°44′48.8″N, 108°18′56.9″–108°19′58.4″E) is located in Huanjiang County of northwest Guangxi, southwest China (Fig. 1a). It is a typical small karst catchment, with an area of 1.14 km^2 (Fu et al., 2015a). It is characterized by a flat depression surrounded by mountains. The average annual precipitation is 1389 mm and the average annual temperature is 18.5 °C. Large rock outcrops are widespread in the catchment without superficial deposits. Spatial distribution of vegetation is heterogeneous, including forestland, shrubland, shrub-grassland and farmland (Fu et al., 2015b).

The studied aquifer is mainly constituted of middle and late Carboniferous dolomite, underlain by an early Carboniferous sandstone aquifer acts as a relatively impermeable layer (Fig. 1b). The superficial deposits are loose and rocky with high hydraulic conductivity (Chen et al., 2011; Fu et al., 2015a). Most of the rainfall

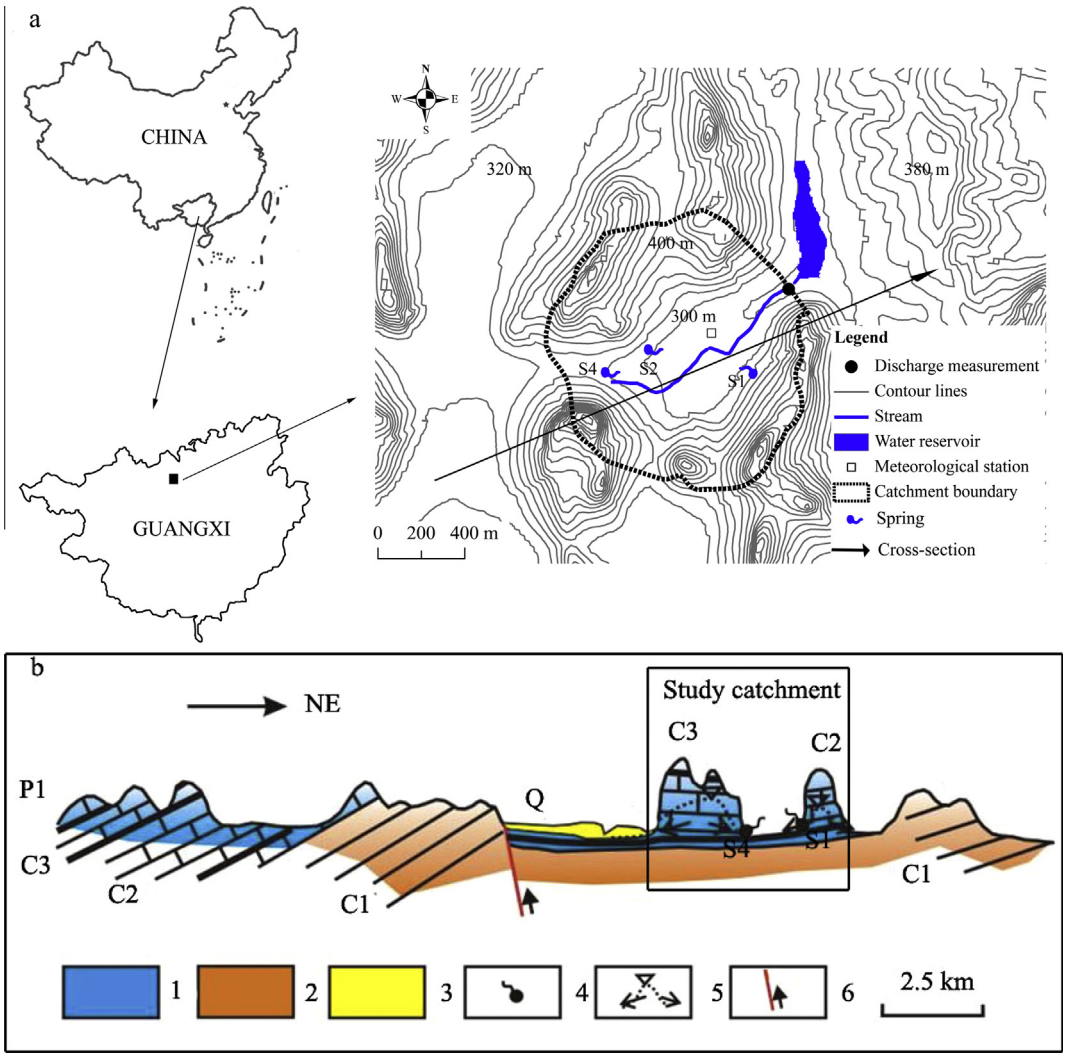

Fig. 1. Location of the study area (a) and geohydrologic background around the study catchment (b). The numbers 1 to 6 mean karst aquifer, sandstone aquifer (relatively impermeable layer), porous quaternary aquifer, spring, ground water flow paths, and fault, respectively. P1 means early Permian and Q means Quaternary, C1, C2, and C3 mean early, middle and late Carboniferous, respectively. S1, S2 and S4 stand for the location of the three springs in the study catchment.

infiltrates to the underground system, and the surface runoff coefficient is always lower than 5% on the hillslope (Chen et al., 2012). Three epikarst springs, all of which flow only in rainy season, are scattered at the foot of the slopes in the catchment. A perennial stream flows from southwest to northeast, and flows into a water reservoir to the northeast of the catchment (Fig. 1a). The average water table depth is about 1 m in the rainy season and more than 3 m in the dry season (Chen et al., 2012). As can be seen from the contour lines and the ground water flow path, the study catchment is closed for both the surface and the underground, and water in the aquifer was only drained by the stream (Fig. 1a and b). Therefore, the stream discharge may reflect the overall characteristics of the aquifer above the outlet (280–640 m a.s.l.), including the soil layer, the epikarst layer and the underlain massive compact dolomite.

2.4. Data obtaining

2.4.1. Precipitation and discharge measurement

A meteorological station, which records the data automatically every 1 h, is located in the center of the catchment to measure the precipitation. A V-notch weir is built in the outlet of the catchment to measure the stream discharge (Fig. 1a). The length of the channel is 5 m and the width is 0.8 m. The height of the triangular-notch weir is 0.35 m. The water level in the weir is measured with a pressure transducer (PS1000, Greenspan Technology, Australia), which records the water level every half hour (Hu et al., 2015). Then the discharge is calculated by water head in the V-notch weir (Mande et al., 2014; Schmidt and Clark, 2012). The instrument is calibrated before the data are analyzed (Fig. 2). The slope of the regression line is 1.012, and R^2 is 0.992, indicating a reliable measurement of the instrument. Then, the modified Maillet, Mangin, and Boussinesq models were used to simulate the stream discharges after six rainfall events chosen from a hydrological year (from Jun., 2013 to Jun., 2014). Other two discharge events after the rainfall on Nov. 7, 2014 and May 25, 2015 were used to verify the models.

2.4.2. The measurement of effective porosity of matrix

Soils in the study area are always thin and even missing in some patches. Compared to the thick dolomite aquifer, the n_{eff} of soils can be neglected. Therefore, the n_{eff} of the rock could be approximate to the n_{eff} of the matrix. Two profiles, about 400 cm depth, were dug with an excavating machine. Two duplicate rock samples with diameters of about 5–10 cm were collected for each layer, every 20 cm from the top to the bottom. The rock samples were taken to the laboratory and the $n_{eff\text{-}m}$ were measured with

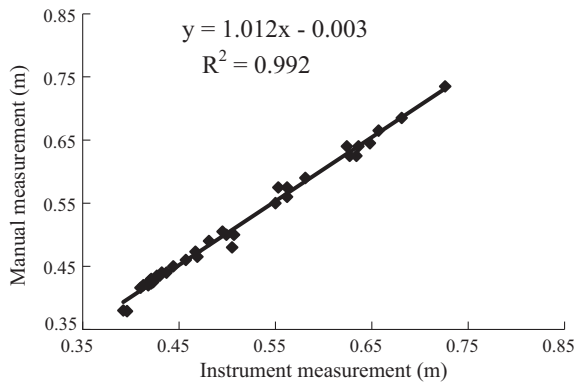

Fig. 2. The calibrating of the instrument for water level measurement.

saturation and buoyancy method (Kurtulus et al., 2012; Yavuz et al., 2013).

3. Results

3.1. Precipitation and stream discharge in a hydrological year and the characteristics of the selected rainfall events

The total precipitation in the studied hydrological year (Jun. 2013 to Jun. 2014) was 1288.4 mm. Quick recession process was found followed each rainfall event. However, no significant seasonal recession was found although long dry period appeared from Dec. 17, 2013 to Feb. 15, 2014 (precipitation is low and can be negligible for some rainfall events such as on Jan. 11 and Jan. 13, 2014) (Fig. 3). The average discharge of the stream in the whole hydrological year was 21.55 m^3/h, with the maximum value of 456.11 m^3/h and the minimum of only 0.67 m^3/h.

An ideal discharge recession process always appears in a long dry period without rainfall (Bonacci, 1993). Therefore, six rainfall events, after which no rainfall event happened until the discharge decreased to the baseflow, were chosen to analyze the recession process of the stream discharge. The monthly precipitations before the selected rainfall events ranged from 99.5 to 278.5 mm. The total precipitations of the selected six rainfall events were from 17.5 to 68 mm. Except May 11 and 18, 2014, when the rainfall intensity data were missing for the problem of the instrument, the maximum rainfall intensities ranged from 4 to 25.5 mm/h, and the maximum and minimum average intensity was 2.48 and 1.46 mm/h, respectively (Table 1). The maximum stream discharges after the selected rainfall events ranged from 95.2 to 824.8 m^3/h, and the minimum discharges ranged from 3.9 to 28.4 m^3/h. The mean discharges of the stream after the rainfall events were from 22.7 to 92.4 m^3/h. Hourly precipitation and discharge data were shown in Fig. 4. A clearly fast and then slow recession process can be found for the discharge after each rainfall event.

3.2. Characteristics of the stream hydrographs after the selected six rainfall events using modified Maillet, Mangin and Boussinesq models

Based on the modified Maillet equation, three exponential components could be seen clearly, which could represent the flow from conduit, fracture and matrix, respectively after the rainfall events on Sep. 24, 2013, Apr. 26, 2014 and May 11, 2014. For other rainfall event, conduit recession and even fracture recession were missing for the lower total precipitation or the lower rainfall intensity (Table 1). The Mangin model showed a clearly fast and then slow recession process for the discharge after each rainfall event except the rainfall on Oct. 1, 2013 which had the lowest precipitation and rainfall intensity. The total discharge after each rainfall event was fitted by Boussinesq model in which a smooth recession curve was found for each recession process (Fig. 5).

The parameters of the three models for simulating the discharges after the six rainfall events were shown in Table 2. For the modified Maillet model, the recession time ranged from 5 to 11 h for the conduit and 35 to 70 h for the fracture. The recession coefficients of the conduit ranged from 0.2441 to 0.5027 h^{-1}, which were about two orders of magnitude higher than that of the baseflow. For the Mangin equation, the infiltration process of the six rainfall events lasted from 13 to 36 h and the infiltration velocities were in the same order of magnitude, ranging from 0.028 to 0.077 h^{-1}. But the variation of flow heterogeneity was higher with a maximum value of 0.655 h^{-1} and a minimum of 0.045 h^{-1}. For the Boussinesq equation, the recession coefficients ranged from 0.0158 h^{-1} to 0.1518 h^{-1}, which was higher than the baseflow recession coefficients of modified Maillet and Mangin equation (Table 2).

Outliers of the calculated parameters in Table 2 were deleted, and then the average values were used to obtain the final equations of the three models (Table 3). For the modified Maillet model, the recession coefficient decreased from conduit to matrix by two orders of magnitude. The recession time for the conduit and fracture were 10 h and 51 h, respectively. For the Mangin model, the infiltration influence period was 20 h.

3.3. Verifications of the modified Maillet, Mangin and Boussinesq models

The discharges of the stream in our study catchment after two Rainfall events, on Nov. 7, 2014 and May 25, 2015, with abundant precipitation followed by a long period without rainfall were used

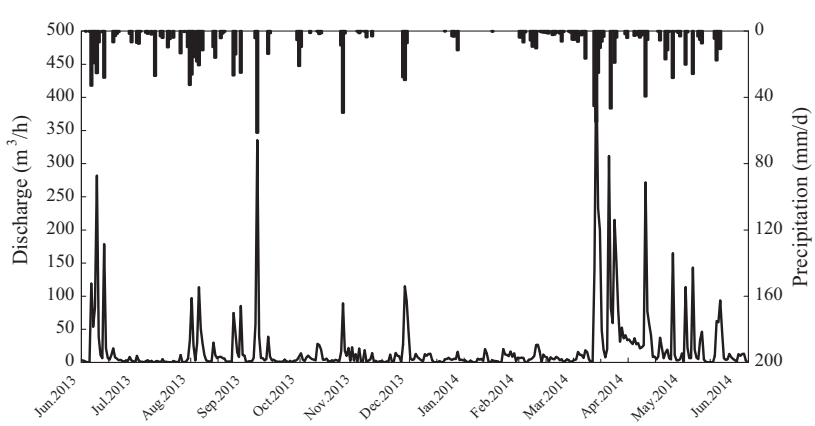

Fig. 3. Precipitation (bars) and stream discharge (solid line) in a whole hydrological year, from Jun. 2013 to Jun. 2014.

Table 1
Characteristics of the rainfall events and stream discharge.

Date	Pre-precipitation[a] (mm)	Total precipitation (mm)	I_{ave} (mm/h)	I_{max} (mm/h)	Q_{max} (m^3/h)	Q_{min} (m^3/h)	Q_{mean} (m^3/h)
Sep. 24, 2013	137.40	68	2.48	12.5	824.8	7.3	47.3
Oct. 1, 2013	163.10	17.5	1.46	4	95.2	7.4	33.2
Nov. 11, 2013	99.50	61	1.5	6	161.0	3.9	22.7
Apr. 26, 2014	278.80	39.5	1.72	25.5	840.6	28.4	92.4
May 11, 2014	162.00	28.3	–	–	436.8	9.9	27.0
May 18, 2014	146.6	20.9	–	–	347.7	12.1	33.5
Nov. 7, 2014	83.2	88.1	–	–	602.2	12.3	45.7
May 25, 2015	75.1	61.3	–	–	284.7	5.9	30.8

[a] Note: Pre-precipitation means the total precipitation of one month (30 d) before the studied rainfall event. I_{ave} means the average rainfall intensity; I_{max} means the maximum rainfall intensity. Q_{max}, Q_{min}, and Q_{mean} mean the maximum, minimum and mean discharge after the rainfall event. – means missing data for the instrument problem. Discharge of Nov. 7, 2014 and May 25, 2015 were used to verify the models, and others were used for the model simulation.

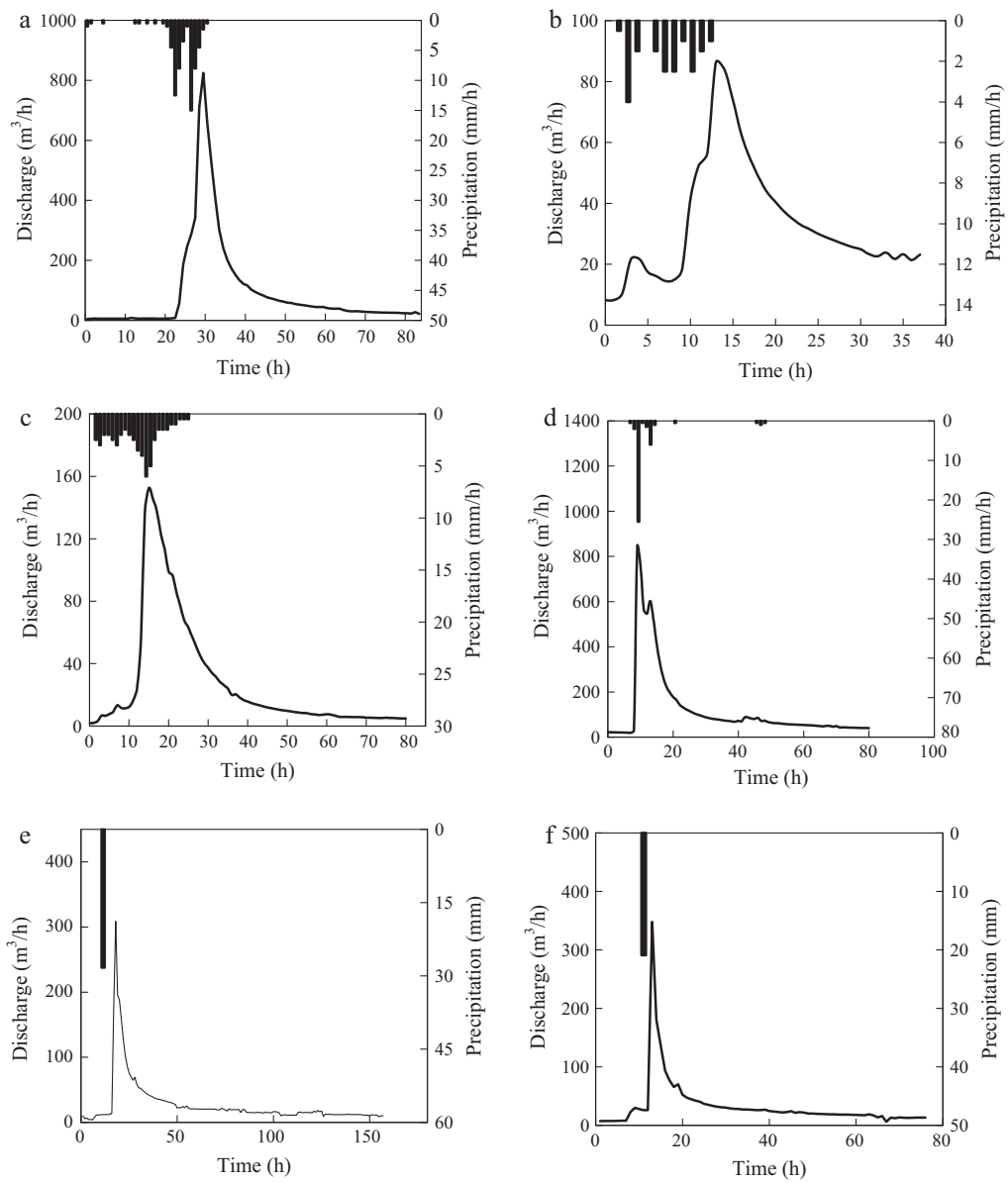

Fig. 4. The hourly discharge (solid line) and precipitation (bars) for the rainfall events on Sep. 24, 2013 (a), Oct. 1, 2013 (b), Nov. 11, 2013 (c), Apr. 26, 2014 (d), May 11, 2014 (e), and May 18, 2014 (f). For (e) and (f), the hourly precipitation data were missing for the instrument problem, and the total precipitation was shown for each rainfall event.

to verify the three models (Fig. 6). It is a pity that the hourly precipitation data of the two verified events were missing because of measurement problems. But the pre-precipitation and the total precipitation could be obtained by manual measurement (Table 1). The mean discharges of the stream after the two verified rainfall events were 45.6 and 30.8 m^3/h, respectively. For both of the rainfall events, the modified Maillet model had the best fitness to the discharge. Mangin model always overestimated the discharge, except

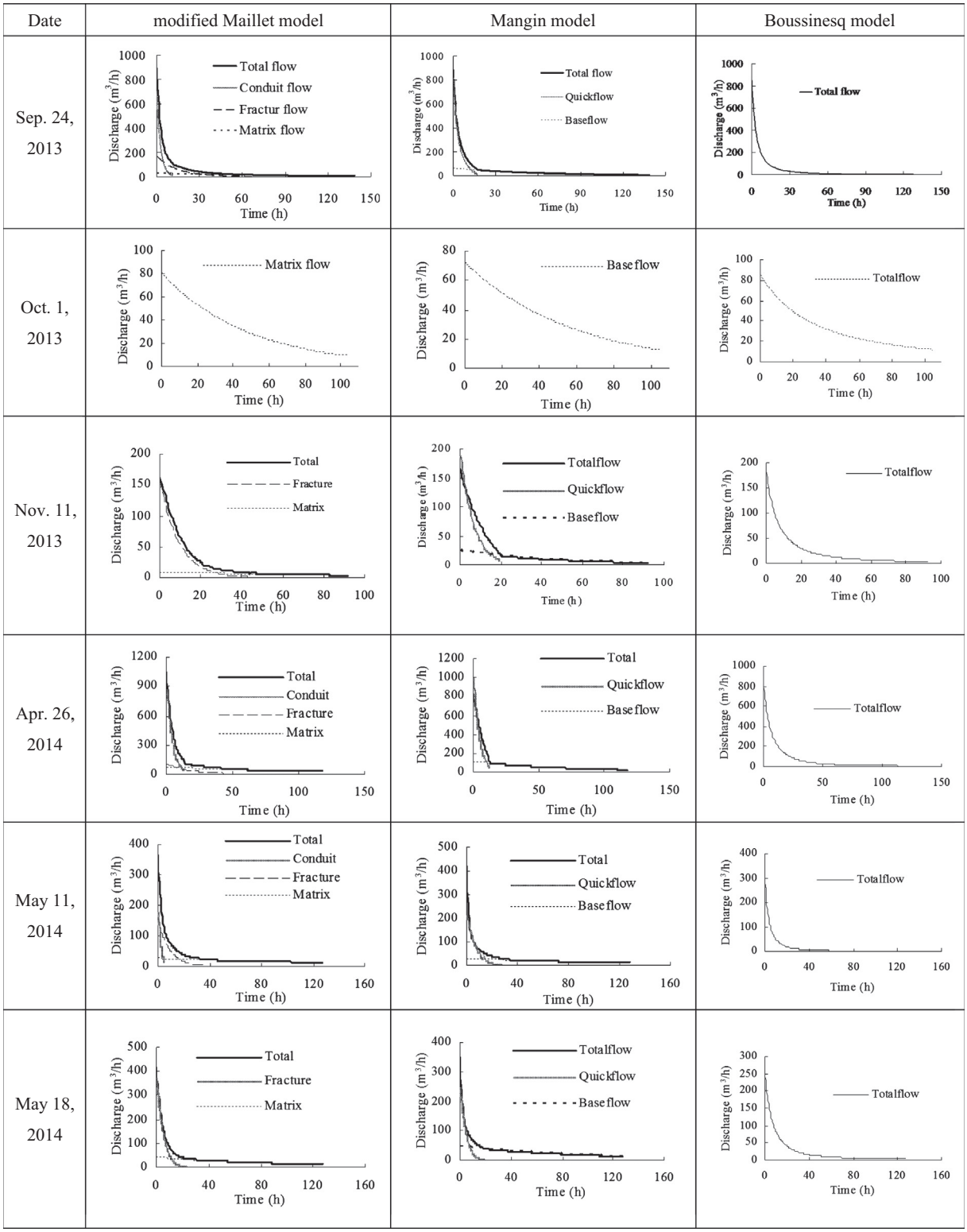

Fig. 5. Simulations of the stream discharge after the selected rainfall events by modified Maillet, Mangin, and Boussinesq models.

the first 20 h. However, Boussinesq model always underestimated the discharge during the whole recession process (Fig. 5a and b).

3.4. The aquifer characteristics deduced by the modified Maillet model

As aforementioned, the modified Maillet model was more suitable for the study catchment. Therefore, this model was used to deduce the aquifer characteristics and the water storage capacity.

3.4.1. The effective porosities of conduit, fracture, and matrix

No obvious trend of $n_{\text{eff-}m}$ was found in the profile 1. However, in the profile 2, $n_{\text{eff-}m}$ decreased with increasing depth in 0–85 cm depths, but had little variation in 85–400 cm depths (Fig. 7). Although the trends of $n_{\text{eff-}m}$ were different in the two profiles, the variations were low, which ranged from 1.67% to 6.50% in the profile 1, and from 1.73% to 7.42% in the profile 2 (Table 4). As a consequence, the $n_{\text{eff-}m}$ could be calculated by the average of the

Table 2
Parameters of the modified Maillet, Mangin, and Boussinesq models for simulating the stream discharge in the six rainfall events.

Date	Modified Maillet model								Mangin model						Boussinesq model	
	Q_c (m^3/h)	t_c (h)	α_c (h^{-1})	Q_f (m^3/h)	t_f (h)	α_f (h^{-1})	Q_m (m^3/h)	t_m (h)	α_m (h^{-1})	α (h^{-1})	Q_b (m^3/h)	Q_q (m^3/h)	H (h^{-1})	ε (h^{-1})	t (h)	α (h^{-1})	Q_0 (m^3/h)
Sep. 24, 2013	697.6	11	0.3807	165.49	70	0.0693	28.33	>70	0.0097	0.0167	59.198	820.65	0.056	0.350	18	0.1518	852.68
Oct. 1, 2013	–	–	–	–	–	–	80.88		0.0209	0.0169	71.969	–	–	–	–	0.0158	85.59
Nov. 11, 2013	–	–	–	158.75	48	0.1128	9.42	>48	0.01	0.0234	24.819	140.21	0.049	0.048	20	0.0741	183.03
Apr. 26, 2014	873.09	13	0.2441	102.91	60	0.0568	72.17	>60	0.0082	0.0129	111.07	707.08	0.077	0.045	13	0.0873	868.11
May 11, 2014	180.02	5	0.5027	158.43	40	0.1151	25.47	>40	0.0059	0.0076	30.96	392.80	0.028	0.655	36	0.1165	335.11
May 18, 2014	–	–	–	370.06	35	0.2097	41.97	>35	0.0098	0.011	46.94	304.43	0.050	0.509	20	0.0777	261.83

two profiles, which is 3.33%. Base on Eqs. (8) and (9), $n_{\text{eff-}c}$ and $n_{\text{eff-}f}$ were calculated to be 0.07% and 0.33, respectively. Then, the percentages of the n_{eff} were 1.88% for conduit, 8.85% for fracture, and 89.27% for matrix (Table 5).

3.4.2. Water storage capacity of the conduit, fracture and matrix

The initial condition with a more saturated aquifer and a higher stream discharge was more ideal for the recession processes and water storage analysis. Both of the rainfall events on Sep. 24, 2013 and on Apr. 26, 2014 were suitable with higher precipitation and stream discharge (Table 2). However, the rainfall on Apr. 26, 2014 was scattered and resulted in a fluctuated recession curve (Fig. 4), which could change the recession process and bring some errors in the calculation. Therefore, water storage capacity of the aquifer was estimated based on the discharge after the rainfall event on Sep. 24, 2013. The maximum volumes of water drained by the three media (conduit, fracture and matrix) were 1804.6, 2369.3, and 2920.6 m^3, respectively. The conduit system drained 25.43% of the total volume in the first 11 h. The water drained from the matrix increased steadily with time and its volume was the highest which accounted for 41.17% of the total volume (Table 5). About half of the water was drained in the first 11 h (Fig. 8) indicating a fast hydrological process.

When the aquifer is saturated, i.e. all the effective porosities are filled with water, the water storage of the aquifer can be estimated by multiplying aquifer thickness and the n_{eff}. As no aquifuge is found in the aquifer above the outlet (Fig. 1b), the assumption is made that the discharge from the outlet reflects the characteristics of the aquifer above the outlet. Then the thickness of the considered aquifer can be estimated by the elevation. The average elevation is 354 m and the elevation of the outlet is 280 m (Fig. 1a). Then, the average thickness of the studied aquifer is calculated to be 74 m. Therefore, the saturated water storage was 51.8, 244.2 and 2464.2 mm for the conduit, fracture and matrix, respectively, and 2700 mm for the total aquifer (Table 5).

3.5. Time series analysis of the discharge data in both year and rainfall event scales

The ACF, for the year scale, had a maximum value of 0.6, and rapidly dropped down to 0.18 in the fifth day. Then it decreased slowly, and fluctuated around 0 at last. This indicated a fast recession of the stream discharge and a well developed karst system. In the rainfall event (68 mm precipitation) scale, the ACF varied more smoothly, with a steep slope in the first 11 h, and a gentle slope in the following time. The memory times of the aquifer for the year and rainfall event scales were 4 days and 8 h, respectively (Fig. 9). The CCF had a delay time of 1 day in year scale, indicating that the average response time of the aquifer to the rainfall was 1 day within a hydrological year. However, in the rainfall event (68 mm precipitation) scale, the delay time was only 1 h, suggesting a very fast response of the aquifer to the rainfall. The cross-correlogram had a steep slope in the first 4 days in the year scale and 10 h in the rainfall event scale, which was similar to that of the auto-correlation analysis.

4. Discussions

4.1. Comparison of modified Maillet, Mangin and Boussinesq recession models in the study catchment

The modified Maillet model is always used in homogeneous aquifers (Bonacci, 1993; Dewandel et al., 2003; Fiorillo, 2014; Tallaksen, 1995). However, it provides the best results in our study catchment which has a heterogeneous aquifer. This suggests that

Table 3
The formular of the three models and their parameters.

Model	Formula	The separation time of hydrograph (h)
Modified Maillet model	$Q_t = Q_1 e^{-0.3758t} + Q_2 e^{-0.0804t} + Q_3 e^{-0.0079t}$	$t_1 = 10$, $t_2 = 51$
Mangin model	$Q_t = Q_q \times \frac{1-0.052t}{1+0.321t} + Q_b e^{-0.0148t}$	$t = 20$
Boussinesq model	$Q_t = \frac{Q_0}{(1+0.0872t)^2}$	–

Note: For symbols see text.

the studied aquifer could be considered as several parallel reservoirs which contribute to the stream discharge independently (Bailly-Comte et al., 2010; Forkasiewicz and Paloc, 1967). For each of the reservoirs, i.e. conduit, fracture, and matrix (Ford and Williams, 2007; Katsanou et al., 2015), it can be regarded as homogeneous, and a sum of exponential components provides better results. Some researchers had the opinion that the quickflow (conduit flow) may follow a linear decrease (Bailly-Comte et al., 2010; Malík and Vojtková, 2012; Schmidt et al., 2014). Fiorillo (2011) used a tank reservoir to simulate this process, and concluded that the reservoir would be linear decrease when the flow was free without energy loss, but could be exponential decrease when the flow recession was an energy loss process. Actually, in our study catchment, conduits are always filled with weathered material. The friction cannot be ignored and the energy is lost during the recession. Therefore, the quick flow can be simulated with exponential recession model.

Dewandel et al. (2003) compared the Maillet and Boussinesq models, and they found Boussinesq equation provided better results but Maillet equation always overestimated the discharge especially in the "influenced" stage. However, they also referred that the Maillet equation was more suitable for an aquifer with a

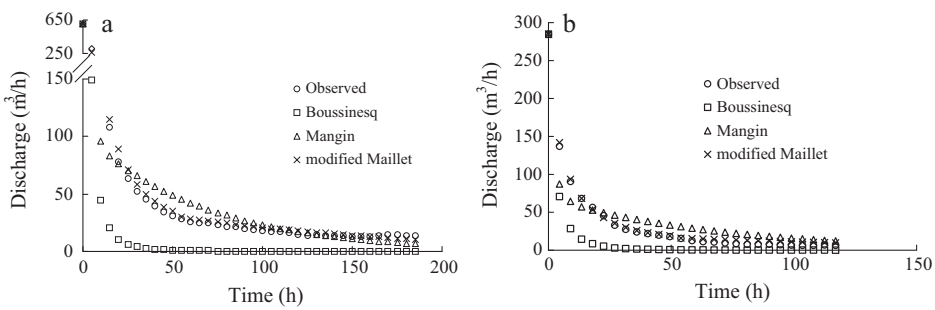

Fig. 6. The validation of modified Maillet, Mangin and Boussinesq models by the stream discharge after the rainfall event on Nov. 11, 2014 (a) and May 25, 2015 (b).

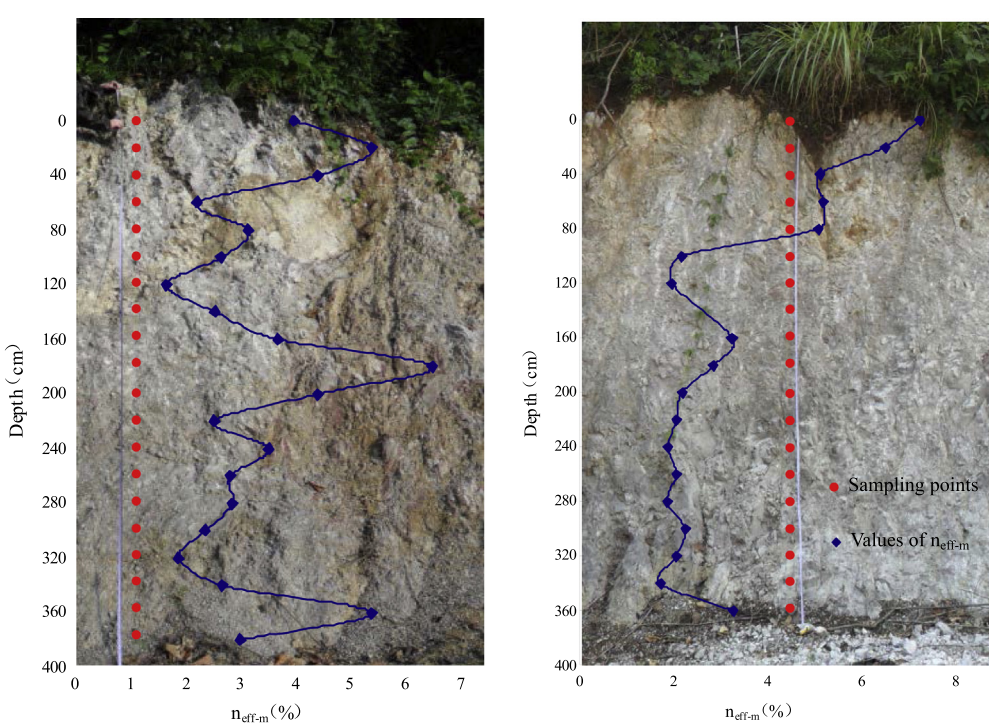

Fig. 7. Effective porosity of the matrix in two profiles. Red points mean the sampling points and the blue points mean the effective porosity value of each point. (For interpretation of the references to color in this figure legend, the reader is referred to the web version of this article.)

Table 4
Effective porosity of matrix in two profiles.

	N	Minimum (%)	Maximum (%)	Standard Deviation (%)	Mean (%)
Profile 1	20.00	1.67	6.50	1.28	3.39
Profile 2	19.00	1.73	7.24	1.70	3.27

Note: *N* means number of sampling points.

Table 5
The characteristic of the studied karst aquifer.

Types	Volume (m^3)	Percentage (%)	n_{eff} (%)	Percentage (%)	Saturated water storage (mm)
Conduit	1804.6	25.43	0.07	1.88	51.8
Fracture	2369.3	33.40	0.33	8.85	244.2
Matrix	2920.6	41.17	3.33	89.27	2464.2
Total	7094.5	100	3.73	100	2760.2

Note: The n_{eff} means effective porosity.

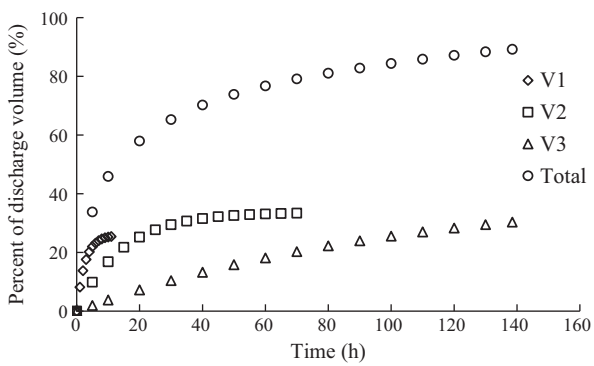

Fig. 8. Percentage of water volume drained by conduit (V1), fracture (V2), matrix (V3), and the total aquifer after the rainfall on Sep. 24, 2013.

thick part under the outlet. In our study catchment, a thick aquifer may locate under the outlet of the catchment. This could also be the reason why the modified Maillet model provides better results. Mangin model was developed for karst aquifer with a dual system including fast and slow water flow (Mangin, 1975), and it was well used in karst aquifer (Eisenlohr et al., 1997; Padilla et al., 1994). However, it overestimates the discharge in our study area. This may be caused by the relatively higher proportion of the intermediate hydraulic conductivity media (fractures) (Table 5).

Although the modified Maillet model provides good results in simulating the stream discharge, and is used in our article to deduce the aquifer structure, it must be acknowledged that there exist questions when this method is used in karst areas. For example, Eisenlohr et al. (1997) gave detailed reasons for the misunderstanding of the separation of the hydrograph, and concluded that the recession of the baseflow was influenced by the total aquifer, not only the matrix. Bailly-Comte et al. (2010) found that the exchange of water between conduit and matrix could control the flow regime of the spring. More recently, Schmidt et al. (2014) found the conduit restrict karst aquifer had a unique flow process. Although numerous questions have been pointed out in the analysis of the hydrograph, the deduced aquifer structure and the related hydrological processes still have their significance, at least in providing an actual phenomenon and guiding the management of water resources (Fiorillo, 2014).

4.2. Recession coefficient of the stream in the modified Maillet model

Recession coefficient always decreases with increasing time (Table 3). However, different results have been found by different researchers. For example, Bonacci (1993) showed that the recession coefficient could increase with increasing time, which was probably caused by the caves or poljes. Schmidt et al. (2014) also found a convex recession curve and they interpreted this by the conduit restricted system. In our study area, no caves or poljes are found, and the conduits may be well connected. As a result, the recession coefficient conventionally decreased in the three phases. The number of the flow phases mainly depends on the degree of karstification. Li (2009) studied three karst springs in southwest China and found three flow phases in two springs and only two phases in the other one. They pointed out that this spring was characterized by matrix and fracture only. In our study area, three phases of recession have been found, indicating that the studied aquifer was characterized by a complex system with conduit, fracture and matrix. However, for a well karstified aquifer with conduit, fracture and matrix systems, not all rainfall could result in three flow regimes of the discharge (Fig. 5 and Table 2). They may appear under the following two conditions. One is that

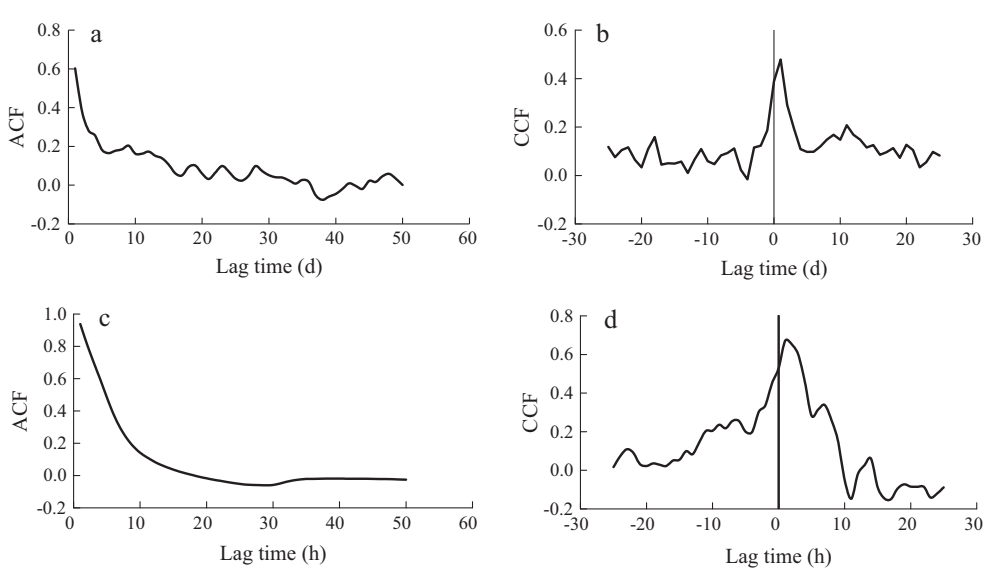

Fig. 9. Auto-correlation and cross-correlation function of the stream discharge in one year scale (a and b), and rainfall event (68 mm) scale (c and d).

the rainfall event has a high precipitation which may saturate the aquifer including the fracture and the conduit systems. The other is that the rainfall event has a high intensity which makes the water reach the fracture and conduit immediately. Therefore, the rainfall can influence the calculation of the recession coefficients.

The above analysis about the recession coefficient is based on the simplified assumption that the recession coefficient is time independent (Fiorillo, 2011). However, it is not always constant even in the same flow regime. Padilla et al. (1994) presented that the recession coefficient varied continuously with time. This may be caused by the change of hydraulic or geometric characteristics of the aquifer during the depletion process (Fiorillo, 2011). The changes of recession coefficient provide significant information about water supply especially during drought period. When the recession coefficient decreased continuously with time, the decrease of the discharge is slower than the exponential recession. Then the aquifer provides more available water during long dry periods. In contrast, when the recession coefficient increases with time, a more rapid decrease of discharge was found and little available water can be supplied (Fiorillo et al., 2012). As can be seen, the knowledge of recession coefficient is very helpful in water management.

4.3. The structure of the studied karst aquifer

Various $n_{\text{eff-}t}$ values of the karst aquifer have been reported. It was 0.1–1% for Bonacci (1993), 2–7% for Delbart et al. (2014), and 5% for Fiorillo et al. (2015). Compared to these results, our study catchment may have a moderate karstification degree with the $n_{\text{eff-}t}$ of 3.73% (Table 4). The $n_{\text{eff-}c}$ is only 0.07% (Table 4) which is much lower than that of Schmidt et al. (2014) who obtained a value of 0.4%. This indicates that the conduit network is not very developed in our study catchment, that is in accordance with our previous study in which long mean residence time, indicating fewer conduits, was found for the studied stream (Hu et al., 2015). However, from the point of view of discharge volume, the conduits drained more than a quarter of the total water volume (Table 5). The proportion of the water drained by different media varies in different areas. Amit et al. (2002) found that the ratio of baseflow volume (matrix storage) to the total storage volume is larger than 80% in northern Israel. Padilla et al. (1994) found the baseflow accounted for 100%, 91%, 90% and 40% of the total volume, respectively for four karst springs in southeast Spain. Li (2009) studied three karst springs and found two of them had higher storage value for the fracture and the other one had higher storage capacity for the matrix in southwest China. As can be seen, this proportion varies irregularly even in the same region. In summary, compared our results with these studies, it can be concluded that the conduit system, in our study catchment, is an important water transmissive media, even though it is not very developed with lower n_{eff}. This indicated that the conduits system in the catchment had high connectivity.

Although the method of integrating the discharge equation over the time from 0 to t_0 (or infinity) could estimate the water storage capacity, it also has been questioned. For example, it may underestimate or overestimates the water volume of drought-resistant or drought-vulnerable springs when the recession coefficient varies with time (Fiorillo, 2014; Fiorillo et al., 2012). In addition, it reflects nothing about the water volume which is below the outlet level (Kiraly, 2002). Despite the problems with this method, it is still very useful in reflecting the water drainage capacity after a rainfall event, especially when other data are missing.

In addition, water storage capacity calculated by the integration method varies from event to event, because the initial discharge is always different caused by different precipitations (Amit et al., 2002). Unlike this method, saturated water storage, which is an intrinsic property and not different under various rainfall conditions, could reflect the maximum water that the aquifer can store. The saturated water storage of the aquifer was 2760.2 mm (Table 5), which is about two times of the average annual precipitation. However, relatively little available water, i.e. the water drained through the outlet, can be used by human (Table 5). This indicated that karst aquifer has a high potential for water supply, but the available water that the aquifer actually provides is low. This may be caused by the high evapotranspiration and, as well, the high proportion of water seeping into the deep aquifer under the outlet. This part of water was lost and cannot be used.

4.4. ACF and CCF in time series analysis

Extremely different results of ACF and CCF have been obtained in the year scale and rainfall event scale analysis (Fig. 9). Long time scale reflects the "average" behavior of the aquifer and event scale shows the system reaction after a single rainfall event. Important information may be lost for the long time scale analysis compared to the event scale, just like Mayaud et al. (2014) who found similar memory effects of two subcatchments in longer time scale but quite different in shorter time scale. In addition, Labat et al. (2000) also found different results of ACF in daily and half hourly scales. Therefore, there is no meaning to compare the time series analysis results of different time scales. However, both of the results showed a steep slope in the auto-correlogram (Fig. 9a and c), which always indicated a high karstification degree of the aquifer with rapid infiltration and fast drainage (Gárfias-Soliz et al., 2010; Lo Russo et al., 2014).

The delay time both in longer time scale (1 d) and shorter time scale (1 h) presents to be short (Fig. 9b and d), indicating a quick response of the aquifer to an input signal in our study catchment. This may result from two reasons. On one hand, our study catchment is much smaller (1.14 km^2). Longer response times were always found in large systems than in small ones, and the longer time was needed to transmit the input impulse to the output (Fiorillo, 2011; Kovačič, 2010). On the other hand, the conduit system may have a well connectivity as deduced by the hydrograph, which results in a shorter lag time (Katsanou et al., 2015). In summary, CCF of both scales showed a fast transmitting from the rainfall to the discharge.

Although the hydrograph analysis and the time series analysis reflect the aquifer structure in different point of view, similar results have been obtained that the studied karst catchment has a quick response to the rainfall. For example, the drainage time of the conduit deduced by the modified Maillet model is about 10 h (Table 3). The lag time of the steep slope of the auto-correlogram, which could reflect the influence of the conduit (Panagopoulos and Lambrakis, 2006), is also about 10 h (Fig. 9c). This indicated that the results obtained from the two methods are reliable.

5. Conclusions

Three recession models were evaluated for simulating stream discharge, and the modified Maillet model was found to be more suitable than Mangin and Boussinesq models in the study catchment. This is because that the studied aquifer can be clearly divided into three hydraulic conductivity components (conduit, fracture and matrix), each of which drained water followed an exponential formula. The effective porosity of the conduit was small (two orders of magnitude lower than that of the matrix), indicating a poorly developed conduit network. However, based on the study of the discharge after a 68 mm rainfall event, the water drained by the conduit system reaches 25.43% of the total

volume, which is very high considered its low effective porosity. This suggests a good connectivity of the conduit network. A great percentage of water is drained by the aquifer in the first 11 h. Therefore, the early recession stage after rainfall should be paid more attention to in water management of the small karst catchment. Both auto-correlogram and cross-correlogram showed a steep slope in short lag times, suggesting a well developed drainage system after the rainfall event. The aquifer characteristics deduced by the hydrograph analysis and time series analysis methods were similar, indicating reliable results of our study. The above results are helpful for further study of the hydrological processes and water resources control in the small catchment in karst regions.

Acknowledgements

This research was supported by the National Key Basic Research Program of China (2015CB452703) and the National Natural Science Foundation of China (41171187 and 51379205). We are also grateful to the three anonymous reviewers for their helpful comments and suggestions.

References

Amit, H., Lyakhovsky, V., Katz, A., Starinsky, A., Burg, A., 2002. Interpretation of spring recession curves. Ground Water 40 (5), 543–551.
Aquilina, L., Ladouche, B., Dorfliger, N., 2006. Water storage and transfer in the epikarst of karstic systems during high flow periods. J. Hydrol. 327 (3–4), 472–485.
Bailly-Comte, V., Jourde, H., Roesch, A., Pistre, S., Batiot-Guilhe, C., 2008. Time series analyses for Karst/River interactions assessment: case of the Coulazou river (southern France). J. Hydrol. 349 (1–2), 98–114.
Bailly-Comte, V., Martin, J.B., Jourde, H., Screaton, E.J., Pistre, S., Langston, A., 2010. Water exchange and pressure transfer between conduits and matrix and their influence on hydrodynamics of two karst aquifers with sinking streams. J. Hydrol. 386 (1–4), 55–66.
Bonacci, O., 1993. Karst springs hydrographs as indicators of karst aquifers. Hydrol. Sci. J. 38 (1), 51–62.
Boussinesq, J., 1877. Essai sur la théorie des eaux courantes [Theory of Underground Water Flow under a Non-permanent Regime]. Imprimerie nationale.
Boussinesq, J., 1904. Recherches the'oriques sur l'e'coulement des nappes d'eau infiltre'es dans le sol et sur le de'bit des sources. J. Math. Pure Appl. 10, 5–78.
Chang, Y., Wu, J.C., Liu, L., 2015. Effects of the conduit network on the spring hydrograph of the karst aquifer. J. Hydrol. 527, 517–530.
Chen, H.S., Zhang, W., Wang, K.L., Fu, W., 2010. Soil moisture dynamics under different land uses on karst hillslope in northwest Guangxi, China. Environ. Earth Sci. 61 (6), 1105–1111.
Chen, H.S., Liu, J.W., Wang, K.L., Zhang, W., 2011. Spatial distribution of rock fragments on steep hillslopes in karst region of northwest Guangxi, China. Catena 84 (1–2), 21–28.
Chen, H.S., Yang, J., Fu, W., He, F., Wang, K.L., 2012. Characteristics of slope runoff and sediment yield on karst hill-slope with different land-use types in northwest Guangxi. Trans. Chin. Soc. Agric. Eng. 28 (16), 121–126 (in Chinese with English abstract).
Chen, H.S., Nie, Y.P., Wang, K.L., 2013. Spatio-temporal heterogeneity of water and plant adaptation mechanisms in karst regions: a review. Acta Ecol. Sin. 33 (2), 317–326 (in Chinese with English abstract).
Covington, M.D., Wicks, C.M., Saar, M.O., 2009. A dimensionless number describing the effects of recharge and geometry on discharge from simple karstic aquifers. Water Resour. Res. 45 (11), W11410.
Delbart, C., Valdés-Lao, D., Barbecot, F., Tognelli, A., Richon, P., Couchoux, L., 2014. Temporal variability of karst aquifer response time established by the sliding-windows cross-correlation method. J. Hydrol. 511, 580–588.
Dewandel, B., Lachassagne, P., Bakalowicz, M., Weng, P., Al-Malki, A., 2003. Evaluation of aquifer thickness by analysing recession hydrographs. Application to the Oman ophiolite hard-rock aquifer. J. Hydrol. 274 (1–4), 248–269.
Eisenlohr, L., Király, L., Bouzelboudjen, M., Rossier, Y., 1997. Numerical versus statistical modelling of natural response of a karst hydrogeological system. J. Hydrol. 202 (1–4), 244–262.
El-Hakim, M., Bakalowicz, M., 2007. Significance and origin of very large regulating power of some karst aquifers in the Middle East. Implication on karst aquifer classification. J. Hydrol. 333 (2–4), 329–339.
Farlin, J., Maloszewski, P., 2013. On the use of spring baseflow recession for a more accurate parameterization of aquifer transit time distribution functions. Hydrol. Earth Syst. Sci. 17 (5), 1825–1831.
Fiorillo, F., 2009. Spring hydrographs as indicators of droughts in a karst environment. J. Hydrol. 373 (3), 290–301.
Fiorillo, F., 2011. Tank-reservoir drainage as a simulation of the recession limb of karst spring hydrographs. Hydrogeol. J. 19 (5), 1009–1019.
Fiorillo, F., 2014. The recession of spring hydrographs, focused on karst aquifers. Water Resour. Manage. 28 (7), 1781–1805.
Fiorillo, F., Revellino, P., Ventafridda, G., 2012. Karst aquifer draining during dry period. J. Cave Karst Stud. 74 (2), 148–156.
Fiorillo, F., Petitta, M., Preziosi, E., Rusi, S., Esposito, L., Tallini, M., 2015. Long-term trend and fluctuations of karst spring discharge in a Mediterranean area (central-southern Italy). Environ. Earth Sci. 74 (1), 153–172.
Ford, D.C., Williams, P., 2007. Karst Hydrogeology and Geomorphology. John Wiley & Sons, New Jersey.
Forkasiewicz, J., Paloc, H., 1967. Le régime de tarissement de la Foux de la Vis. Etude preliminaire. Chron. d'Hydrogeol., BRGM 3 (10), 61–73.
Fu, T.G., Chen, H.S., Zhang, W., Nie, Y.P., Gao, P., Wang, K.L., 2015a. Spatial variability of surface soil saturated hydraulic conductivity in a small karst catchment of southwest China. Environ. Earth Sci. 74 (3), 2381–2391.
Fu, T.G., Chen, H.S., Zhang, W., Nie, Y.P., Wang, K.L., 2015b. Vertical distribution of soil saturated hydraulic conductivity and its influencing factors in a small karst catchment in Southwest China. Environ. Monit. Assess. 187 (3), 1–13.
Gárfias-Soliz, J., Llanos-Acebo, H., Martel, R., 2010. Time series and stochastic analyses to study the hydrodynamic characteristics of karstic aquifers. Hydrol. Process. 24 (3), 300–316.
Ghasemizadeh, R., Hellweger, F., Butscher, C., Padilla, I., Vesper, D., Field, M., Alshawabkeh, A., 2012. Review: groundwater flow and transport modeling of karst aquifers, with particular reference to the North Coast Limestone aquifer system of Puerto Rico. Hydrogeol. J. 20 (8), 1441–1461.
Goldscheider, N., Drew, D., 2007. Methods in Karst Hydrogeology: IAH: International Contributions to Hydrogeology. Taylor & Francis, London.
Gregor, M., Malík, P., 2012. Construction of master recession curve using genetic algorithms. J. Hydrol. Hydromech. 60 (1), 3–15.
Hu, K., Chen, H.S., Nie, Y.P., Wang, K.L., 2015. Seasonal recharge and mean residence times of soil and epikarst water in a small karst catchment of southwest China. Sci. Rep. 5, 10215.
Jacob, T., Bayer, R., Chery, J., Jourde, H., Moigne, N.L., Boy, J.-P., Hinderer, J., Luck, B., Brunet, P., 2008. Absolute gravity monitoring of water storage variation in a karst aquifer on the larzac plateau (Southern France). J. Hydrol. 359 (1–2), 105–117.
Jacob, T., Chery, J., Bayer, R., Le Moigne, N., Boy, J.P., Vernant, P., Boudin, F., 2009. Time-lapse surface to depth gravity measurements on a karst system reveal the dominant role of the epikarst as a water storage entity. Geophys. J. Int. 177 (2), 347–360.
Jiang, Z.C., Lian, Y.Q., Qin, X.Q., 2014. Rocky desertification in Southwest China: impacts, causes, and restoration. Earth-Sci. Rev. 132, 1–12.
Katsanou, K., Maramathas, A., Lambrakis, N., 2014. Simulation of karst springs discharge in case of incomplete time series. Water Resour. Manage. 29 (5), 1623–1633.
Katsanou, K., Lambrakis, N., Tayfur, G., Baba, A., 2015. Describing the karst evolution by the exploitation of hydrologic time-series data. Water Resour. Manage. 29 (9), 3131–3147.
Kiraly, L., 2002. Karstification and Groundwater Flow. Evolution of Karst: From Prekarst to Cessation. Zalozba ZRC, Postojna-Ljubljana, pp. 155–190.
Kiraly, L., Perrochet, P., Rossier, Y., 1995. Effect of the epikarst on the hydrograph of karst springs: a numerical approach. Bull. Centre d'Hydrogéol. 14, 199–220.
Kovačič, G., 2010. Hydrogeological study of the Malenščica karst spring (SW Slovenia) by means of a time series analysis. Acta Carsol. 39 (2), 201–215.
Kovács, A., Perrochet, P., 2008. A quantitative approach to spring hydrograph decomposition. J. Hydrol. 352 (1), 16–29.
Kovács, A., Perrochet, P., Király, L., Jeannin, P.Y., 2005. A quantitative method for the characterisation of karst aquifers based on spring hydrograph analysis. J. Hydrol. 303 (1), 152–164.
Kurtulus, C., Bozkurt, A., Endes, H., 2012. Physical and mechanical properties of serpentinized ultrabasic rocks in NW Turkey. Pure Appl. Geophys. 169 (7), 1205–1215.
Labat, D., Ababou, R., Mangin, A., 2000. Rainfall–runoff relations for karstic springs. Part I: convolution and spectral analyses. J. Hydrol. 238 (3–4), 123–148.
Lacey, G.C., Grayson, R.B., 1998. Relating baseflow to catchment properties in south-eastern Australia. J. Hydrol. 204 (1–4), 231–250.
Li, L.L., 2009. Study of Effects of Ecological Environment on Regulated Function of Epikarst Water in Typical Karst Area of Southwest, China. Southwest University, Congqing, China.
Li, S., Ren, H.D., Xue, L., Chang, J., Yao, X.H., 2014. Influence of bare rocks on surrounding soil moisture in the karst rocky desertification regions under drought conditions. Catena 116, 157–162.
Liu, L.H., Shu, L.C., Chen, X.H., Wang, E., Oromo, T., 2010. Rainfall-driven spring hydrograph modeling in a karstic water system, Southwestern China. Water Resour. Manage. 24 (11), 2689–2701.
Lo Russo, S., Amanzio, G., Ghione, R., De Maio, M., 2014. Recession hydrographs and time series analysis of springs monitoring data: application on porous and shallow aquifers in mountain areas (Aosta Valley). Environ. Earth Sci. 73 (11), 7415–7434.
Maillet, E., 1905. Essais d'Hydraulique souterraine et fluviale [Underground and River Hydrology]. Hermann, Paris, 218 pp.
Malík, P., Vojtková, S., 2012. Use of recession-curve analysis for estimation of karstification degree and its application in assessing overflow/underflow conditions in closely spaced karstic springs. Environ. Earth Sci. 65 (8), 2245–2257.

Mande, T., Ceperley, N., Weijs, S.V., Repetti, A., Parlange, M.B., 2014. Toward a new approach for hydrological modeling: a tool for sustainable development in a savanna agro-system. In: Bolay, J.-C., Hostettler, S., Hazboun, E. (Eds.), Technologies for Sustainable Development. Springer International Publishing, pp. 85–98.

Mangin, A., 1975. Contribution à l'étude hydrodynamique des aquiféres karstiques [A contribution to the study of karst aquifer hydrodynamics]. 3éme partie. Ann. Spéléogie 30(1), 21–124.

Mangin, A., 1984. Pour une meilleure connaissance des systèmes hydrologiques à partir des analyses corrélatoire et spectrale. J. Hydrol. 67 (1–4), 25–43.

Mayaud, C., Wagner, T., Benischke, R., Birk, S., 2014. Single event time series analysis in a binary karst catchment evaluated using a groundwater model (Lurbach system, Austria). J. Hydrol. 511, 628–639.

Nie, Y.P., Chen, H.S., Wang, K.L., Yang, J., 2012. Water source utilization by woody plants growing on dolomite outcrops and nearby soils during dry seasons in karst region of Southwest China. J. Hydrol. 420, 264–274.

Padilla, A., Pulido-Bosch, A., 1995. Study of hydrographs of karstic aquifers by means of correlation and cross-spectral analysis. J. Hydrol. 168 (1), 73–89.

Padilla, A., Pulido-Bosch, A., Mangin, A., 1994. Relative importance of baseflow and quickflow from hydrographs of karst spring. Ground Water 32 (2), 267–277.

Panagopoulos, G., Lambrakis, N., 2006. The contribution of time series analysis to the study of the hydrodynamic characteristics of the karst systems: application on two typical karst aquifers of Greece (Trifilia, Almyros Crete). J. Hydrol. 329 (3), 368–376.

Perrin, J., Jeannin, P.Y., Zwahlen, F., 2003. Epikarst storage in a karst aquifer: a conceptual model based on isotopic data, Milandre test site, Switzerland. J. Hydrol. 279 (1–4), 106–124.

Schmidt, C.A., Clark, M.W., 2012. Evaluation of a denitrification wall to reduce surface water nitrogen loads. J. Environ. Qual. 41 (3), 724–731.

Schmidt, S., Geyer, T., Guttman, J., Marei, A., Ries, F., Sauter, M., 2014. Characterisation and modelling of conduit restricted karst aquifers – example of the Auja spring, Jordan Valley. J. Hydrol. 511, 750–763.

Tallaksen, L., 1995. A review of baseflow recession analysis. J. Hydrol. 165 (1), 349–370.

White, W.B., 2003. Conceptual models for karstic aquifers. Speleogenesis Evol. Karst Aquifers 1 (1), 1–6.

Yavuz, H., Tufekci, K., Kayacan, R., Cevizci, H., 2013. Predicting the dynamic compressive strength of carbonate rocks from quasi-static properties. Exp. Mech. 53 (3), 367–376.

Yuan, D.X., 1994. Karstology of China. Geological Publishing House, Beijing.

Zhang, J.G., Chen, H.S., Su, Y.R., Kong, X.L., Zhang, W., Shi, Y., Liang, H.B., Shen, G.M., 2011. Spatial variability and patterns of surface soil moisture in a field plot of karst area in southwest China. Plant Soil Environ. 57 (9), 409–417.